HHS Public Access

Author manuscript

J Immunol. Author manuscript; available in PMC 2019 November 18.

Published in final edited form as:

J Immunol. 2018 March 15; 200(6): 2025–2037. doi:10.4049/jimmunol.1700325.

ILDR2 Is a Novel B7-like Protein That Negatively Regulates T Cell Responses

Iris Hecht[*], **Amir Toporik**[*], **Joseph R. Podojil**[†,‡], **Ilan Vaknin**[*], **Gady Cojocaru**[*], **Anat Oren**[*], **Elizabeta Aizman**[*], **Spencer C. Liang**[§], **Ling Leung**[§], **Yosef Dicken**[*], **Amit Novik**[*], **Nadav Marbach-Bar**[*], **Aziza Elmesmari**[¶], **Clare Tange**[¶], **Ashley Gilmour**[¶], **Donna McIntyre**[¶], **Mariola Kurowska-Stolarska**[¶], **Kay McNamee**[‖], **Judith Leitner**[#], **Shirley Greenwald**[*], **Liat Dassa**[*], **Zurit Levine**[*], **Peter Steinberger**[#], **Richard O. Williams**[‖], **Stephen D. Miller**[†,‡], **Iain B. McInnes**[¶], **Eyal Neria**[*], **Galit Rotman**[*]

[*]Compugen Ltd., Holon 5885849, Israel

[†]Department of Microbiology-Immunology, Feinberg School of Medicine, Northwestern University, Chicago, IL 60611

[‡]Interdepartmental Immunobiology Center, Feinberg School of Medicine, Northwestern University, Chicago, IL 60611

[§]Compugen USA Inc., South San Francisco, CA 94080

[¶]Institute of Infection, Immunity and Inflammation, University of Glasgow, Glasgow G12 8TA, United Kingdom

[‖]Kennedy Institute, Nuffield Department of Orthopaedics, Rheumatology and Musculoskeletal Sciences, University of Oxford, Oxford OX3 7FY, United Kingdom

[#]Division of Immune Receptors and T Cell Activation, Institute of Immunology, Center for Pathophysiology, Infectiology and Immunology, Medical University of Vienna, 1090 Vienna, Austria

Abstract

The B7-like protein family members play critical immunomodulatory roles and constitute attractive targets for the development of novel therapies for human diseases. We identified Ig-like domain–containing receptor (ILDR)2 as a novel B7-like protein with robust T cell inhibitory activity, expressed in immune cells and in immune-privileged and inflamed tissues. A fusion protein, consisting of ILDR2 extracellular domain with an Fc fragment, that binds to a putative counterpart on activated T cells showed a beneficial effect in the collagen-induced arthritis model

Address correspondence and reprint requests to Dr. Iris Hecht, Compugen Ltd., 26 Harokmim Street, Building D, Holon 5885800, Israel. Irish@cgen.com.

Disclosures

I.H., A.T., I.V., G.C., A.O., E.A., Y.D., A.N., N.M.-B., S.G., L.D., Z.L., E.N., and G.R. are employees or former employees of Compugen Ltd. S.C.L. and L.L. are employees of Compugen USA Inc. Research at the laboratory of S.D.M., P.S., R.O.W., and I.B.M. was conducted under research support from Compugen Ltd. S.D.M. and J.R.P. are consultants to Compugen Ltd. I.B.M. is a member of the Compugen Ltd. scientific advisory board. I.H., Z.L., G.R., A.N., A.T., L.D., S.G., S.D.M, J.R.P., E.N., I.B.M., M.K.-S., and A.E. are co-inventors of Compugen-owned intellectual property that includes ILDR2.

The online version of this article contains supplemental material.

and abrogated the production of proinflammatory cytokines and chemokines in autologous synovial-like cocultures of macrophages and cytokine-stimulated T cells. Collectively, these findings point to ILDR2 as a novel negative regulator for T cells, with potential roles in the development of immune-related diseases, including autoimmunity and cancer.

The immune system is tightly regulated by a network of positive and negative immune regulators, including the B7/CD28 family of proteins (1, 2), which belong to the Ig superfamily (IgSF), and play pivotal roles in fine tuning of immune responses and in maintenance of peripheral self-tolerance. The importance of these proteins is further emphasized by their involvement in pathological processes and by their clinical application in a variety of human diseases, including autoimmunity and cancer (3, 4). As a result of their fundamental biological importance and therapeutic potential, there has been considerable interest in the identification of additional members of the extended B7/CD28 family of ligands and receptors.

The human proteome encompasses hundreds of IgSF proteins, yet only a few are key modulatory components of the immune system, and of T cell regulation in particular (4, 5). Proteins of the IgSF tend to evolve quickly (6); therefore, sequence similarity to an annotated member of the IgSF is a poor predictor of its function. To discover novel immune-modulatory proteins, we set to identify remote paralogs of known members of the B7-like family that modulate T cell activity (e.g., programmed death ligand 1 [PD-L1], CD86, B7-H3, B7-H4, and V-domain Ig suppressor of T cell activation [VISTA]), based on similar genomic and proteomic characteristics, such as gene structure, protein domains, predicted cellular localization, and expression pattern, among known B7 family members. Using this search strategy, we identified an IgSF protein family member, known as Ig-like domain-containing receptor (ILDR)2, as a new predicted B7-like protein with potential immunomodulatory function. The experimental work presented in this article confirmed this prediction.

ILDR2 and its two paralogs, ILDR1 and lipolysis-stimulated receptor (LSR; also named ILDR3), have been designated as angulin family proteins (angulin-1/LSR, angulin-2/ILDR1, and angulin-3/ILDR2), following their identification as protein components of tricellular tight junctions (tTJs), which are required for recruitment of tricellulin to tTJs (7). tTJs are specialized structures of tricellular contacts (i.e., where the corners of three epithelial cells meet) that are required for full barrier function of the cellular sheet (8).

Ildr2, the gene encoding the murine ortholog (formerly designated "*Lisch-like*") was originally identified as a modifier of susceptibility to type 2 diabetes in obese mice, and it was associated with reduced β cell mass and replication rates and persistent mild hypoinsulinemic hyperglycemia (9). The human gene encoding ILDR2, originally named C1orf32, is located in a region on Chr1q23–25 that has been associated with type 2 diabetes (9).

Roles in hepatic clearance of lipoproteins and in lipid homeostasis have been described for LSR (10) and for ILDR2 (11). ILDR1 was shown to regulate gastrointestinal hormone

secretion through a mechanism dependent on fatty acids and lipoproteins (12). In addition, involvement in aggressive cancer behavior has been reported for LSR (13).

A recent publication reported upregulation of ILDR2 in human dendritic cell (DC)2 cells, a subpopulation of polarized DCs that promotes Th2 differentiation (14). However, no immune-related function has been reported previously for any of the angulin family members.

In this article, we demonstrate that ILDR2 displays negative-regulatory functions on human and mouse T cells in various experimental systems. Furthermore, a fusion protein of ILDR2 extracellular domain with an Fc fragment (ILDR-Fc), displays therapeutic effects in collagen-induced arthritis (CIA), a mouse model of rheumatoid arthritis (RA). We conclude that ILDR2 represents a novel B7-like ligand that exerts negative immune modulation via interaction with a putative counterpart receptor expressed on activated T cells, thereby defining it as a novel immune checkpoint.

Materials and Methods

Mice

SJL/J mice (Harlan Labs, Indianapolis, IN) and DO11.10 and BALB/c mice (The Jackson Laboratory, Bar Harbor, ME) were housed under specific pathogen–free conditions in the Northwestern University Center for Comparative Medicine. All of the procedures performed on animals within this study were conducted in accordance with the guidelines of the Northwestern University Animal Care and Use Committee. Male DBA/1 mice (Harlan Labs) were used at 8–12 wk of age. All procedures were approved by the Clinical Medicine Ethical Review Board and the UK Home Office.

Bioinformatic analysis of ILDR2

Bioinformatic characteristics, such as genomic structure and splice variant identification, were determined using Compugen’s LEADS platform (15). Prediction for transmembrane domain was performed with TMHMM (16). Signal peptide was predicted with SignalP 4.0 (17) and validated experimentally by N-terminal sequencing. Ig domain identification was performed using InterProScan (18). Secondary structures were predicted using PSIPRED (19) and SCRATCH (20). Multiple sequence alignments were performed with MAFFT (21). EMBOSS-Needle was used on globally aligned sequences to calculate the level of sequence identity and similarity (22, 23). The IgV domains of known B7-related proteins were extracted from Swiss-Prot sequence annotation features (24).

Immunohistochemical analysis

Immunohistochemistry (IHC) was carried out at Rockland Immunochemicals (Gilbertsville, PA) on formalin-fixed paraffin-embedded sections of normal or diseased human tissue samples. Inflammatory bowel disease (IBD) biopsies (two samples of Crohn’s disease and two samples of ulcerative colitis, obtained from US Biomax) were analyzed and compared with samples of normal small intestine and colon. A rabbit polyclonal anti-ILDR2 Ab, Ab-13, was used (at 2.5 μg/ml) as the primary Ab, and the principal detection system

consisted of a secondary Biotinylated Goat Anti-Rabbit IgG Antibody (catalog number BA-1000), a VECTASTAIN ABC-AP Staining KIT (catalog number AK-5000), and a VECTOR Red Alkaline Phosphatase (Red AP) Substrate Kit (SK-5100; all from Vector Laboratories), which was used to produce a fuchsia-colored deposit. Stained slides were imaged with a DVC 1310C digital camera coupled to a Nikon microscope.

FACS and quantitative RT-PCR analyses of ILDR2 expression on immune cells

Human PBMCs were isolated by Ficoll gradient from buffy coats of healthy donors. Monocytes were enriched by negative selection using a RosetteSep Human Monocyte Enrichment Kit (STEMCELL Technologies). To generate macrophages (MΦs), monocytes were cultured in 100 ng/ml M-CSF (R&D Systems) for 5 d.

For FACS analysis, we used CGEN–Ab-28, an anti-ILDR2 human IgG1 mAb identified by phage display, and Synagis (palivizumab, a human IgG1 anti-RSV mAb; Caligor Rx) as isotype control. Each Ab was conjugated to Alexa Fluor 647 using an Alexa Fluor 647 Conjugation Kit (Life Technologies), according to the manufacturer's instructions. Fluorophore-conjugated mAbs against the following human proteins were purchased from BioLegend: Pacific Blue–conjugated anti-CD14, PE-conjugated anti-CD56, and FITC-conjugated anti-HLA-DR. PerCP-Cy5.5–conjugated anti-CD16 was obtained from BD Biosciences. Prior to staining of cells with Ab, Fcγ receptors were blocked by incubating 4×10^5 cells with 400 μg/ml human IgG (Jackson ImmunoResearch) in FACS buffer at 4°C for 30 min. Conjugated Abs were used, at 5 μg/ml in FACS buffer, to stain cells at 4°C for 30 min, followed by two washes in FACS Buffer and analysis using a FACSCanto. Captured data were analyzed with FlowJo software.

For quantitative RT-PCR (qRT-PCR) analysis, RNA was purified from cells using an RNeasy Mini Kit (catalog number 74014; QIAGEN), according to the manufacturer's protocol. cDNA was generated using a High Capacity cDNA Reverse Transcription Kit (catalog number 4368814; Applied Biosystems). cDNA diluted 1:10 (representing 25 ng RNA per reaction) was used as a template for qRT-PCR, using TaqMan Fast Advanced Master Mix (catalog number 4444557; Applied Biosystems) and gene-specific TaqMan probes for human ILDR2 (Hs01025494_m1) and for housekeeping genes (HSKPs; RPL19, Hs01577060_gH and GUSB, Hs99999908_m1; both from Life Technologies). Analysis was performed using the ddCt method. The resulting quantities were normalized using those obtained for the HSKPs.

Ectopic expression of ILDR2 on T cell stimulator cells and T cell activation

Human ILDR2 was ectopically expressed in T cell stimulator cells (hereafter referred to as "stimulator cells"). Briefly, these cells are Bw5147 cells stably expressing a membrane-bound anti-human CD3 single-chain Ab fragment [described in detail by Leitner et al. (25)]. Expression constructs encoding for the long or short ILDR2 isoforms were cloned in the retroviral expression vector pCJK2 and expressed in these stimulator cells. The expression of these isoforms, which have an identical extracellular domain (ECD), was examined by FACS analysis using a specific anti-ILDR2 polyclonal Ab (Ab-13). Cells expressing empty vector and no human costimulatory molecule were used as control. As positive controls for

positive and negative costimulation, stimulator cells expressing a known positive costimulatory protein (ICOSL) or a known coinhibitory protein (PD-L1) were used. The use of ICOSL-, CD70-, or B7-H3–expressing stimulator cells to activate human T cells has been described previously (25-27).

Stimulator cells were irradiated (2 × 3000 rad) and seeded in flat-bottom 96-well plates at 2 × 10^4 cells per well, in the presence of 1 × 10^5 untouched $CD3^+$ human T cells, previously purified from buffy coats derived from healthy donors using Ficoll-Paque (GE Healthcare) and MACS depletion of CD11b, CD14, CD16, CD19, CD33 and MHC class II–bearing cells, as described previously (28). Alternatively, purified $CD8^+$ human T cells were used. After 48 h of coculture with the stimulator cells, T cell proliferation was measured by [^{3}H]thymidine incorporation, as described by Pfistershammer et al. (29).

Production of ILDR2-Fc fusion proteins

ILDR2-Fc fusion proteins were produced by cloning the ECD of human ILDR2 (aa 1–184) fused to the Fc region (C and hinge regions) of mouse IgG2a (ILDR2-mFc) or the ECD of human ILDR2 (aa 1–184) fused to the Fc region (C and hinge regions) of human IgG1 (ILDR2-hFc) in mammalian expression vectors. ILDR2-mFc contains a TEV linker at the ECD–Fc junction. ILDR2-hFc carries a C220S mutation at the hinge domain of human IgG1 Fc. Various batches of these proteins were produced from stable pools of CHO-S cells at Catalent Pharma Solutions (Middleton, WI) or at Cobra Biologics (Södertälje, Sweden). All proteins were produced using fed-batch technology and purified from culture supernatants using standard protein A column affinity chromatography.

Activation of human T cells

Total human PBMCs were obtained from healthy donors' buffy coats by standard density centrifugation using Ficoll-Paque Plus (GE Healthcare). Human naive $CD4^+$ T cells were further isolated using a CD4+ T Cell Isolation Kit II, human (Miltenyi Biotec), according to the manufacturer's instructions. Purified naive human $CD4^+$ T cells were cocultured with previously irradiated autologous PBMCs (at 3000 rad) at a 1:1 ratio (5 × 10^5 T cells with 5 × 10^5 irradiated PBMCs per well) and activated with anti-CD3 Ab (0.5 μg/ml, clone OKT3) and anti-CD28 Ab (2 μg/ml, clone CD28.2; both from eBioscience), in the presence or absence of the stated concentrations of soluble ILDR2-hFc or control Ig (human IgG1; Synagis). The amount of protein in each well was balanced to a total of 10 μg/ml with control Ig. After 24 h in culture, cells were pulsed with [^{3}H]thymidine and were harvested after 72 h in culture. Each sample was tested in duplicate.

An additional human T cell activation assay was carried out using plate-bound proteins: 96-well plates were coated with anti-CD3 Ab (1 μg/ml, clone UCHT-1; R&D Systems) overnight at room temperature, followed by coating with soluble ILDR2-hFc or control Ig (human IgG1; Synagis) at 10 μg/ml for 4 h at 37°C. Purified human bulk ($CD3^+$) T cells were obtained from buffy coats of healthy donors using RosetteSep Human T Cell Enrichment Cocktail (STEMCELL Technologies) and labeled with Cell Proliferation Dye eFluor 450 (catalog number 65-0842-85). The labeled cells were plated in the precoated plates, and anti-CD28 (catalog number 302914; BioLegend) was added in a soluble form to

a final concentration of 2 μg/ml. Cells were collected after 5 d of culture for FACS analysis, and cell proliferation was assessed as the percentage of eFluor 450^{low} cells.

For T cell reactivation, human T cell blasts were generated from PBMCs following stimulation with PHA (2 μg/m) and human IL-2 (4 ng/ml) for 10 d. T cell blasts were harvested and frozen for later use. Anti-CD3 (UCHT-1) was used to coat 96-well plates at 0.5 μg/ml (4°C) overnight. Plates were washed with PBS, and tested proteins were immobilized on the plates at different concentrations. T cell blasts were added at 1×10^5 per well, and supernatants were collected 24 h later for analysis of IL-2 secretion using a Human IL-2 Quantikine kit. Recombinant human PD-L1–Fc (B7-H1–Fc) was used as positive control, and recombinant human IgG1-Fc (both from R&D Systems) was used as negative control. This assay was carried out by R&D Systems.

Activation of murine T cells

Naive $CD4^+$ T cells were isolated from total lymph node and splenocyte populations of wild-type mice (BALB/c or SJL) using an autoMACS cell separator (Miltenyi Biotec; $CD4^-$ sort plus anti-CD25 to remove $CD25^+$ cells from the isolated $CD4^+$ T cells, followed by $CD62L^+$ sort). Polyclonal T cell activation was carried out using naive $CD4^+$ T cells and synthetic beads (Dynabeads M-450 Epoxy; Invitrogen) coated with anti-CD3 (0.5 μg/ml, clone 2C11) and anti-CD28 (2 μg/ml, clone 37.51; both from eBioscience), following the manufacturer's protocol. The beads were coated with the above mentioned mAbs in the presence or absence of the stated concentrations of ILDR2-mFc, or mouse IgG2a (Bio X Cell) as negative control. The total amount of protein used for bead coating was completed with mouse IgG2a (mIgG2a) to 10 μg/ml. $CD4^+$ T cells were activated with the coated beads at a 1:1 ratio in flat-bottom 96-well plates, and cellular proliferation was evaluated by [^{3}H]thymidine incorporation after 72 h in culture.

For Ag-specific T cell activation, naive $CD4^+$ T cells were isolated from spleens of DO11.10 mice (transgenic for an $OVA_{323–339}$-specific TCR; The Jackson Laboratory) using an autoMACS cell separator (Miltenyi Biotec; $CD4^-$ sort plus anti-CD25 to remove $CD25^+$ cells from the isolated $CD4^+$ T cells, followed by $CD62L^+$ sort). Splenocytes from a syngeneic BALB/c mouse were collected in parallel, irradiated with 3000 rad, and used as APCs. Naive DO11.10 $CD4^+$ T cells (0.5×10^6 T cells per well) were cultured with irradiated APCs at a 1:1 ratio in flat-bottom 96-well plates and activated in the presence of $OVA_{323–339}$ peptide (20 μg/ml). Soluble ILDR2-mFc and Ig control (mouse IgG2a; Bio X Cell) were added at the stated concentrations. Cultures were pulsed with 1 μCi of [^{3}H]thymidine at 24 h and harvested at 72 h.

Binding of ILDR2-hFc to resting and activated human T cells

Human primary $CD4^+$ or $CD8^+$ T cells were enriched from healthy donor–derived buffy coats using RosetteSep Human T Cell Enrichment Cocktail (STEMCELL Technologies), according to the manufacturer's instructions. For T cell activation, 96-well plates were coated with PBS in the presence or absence of 1 μg/ml anti-CD3 (clone UCHT-1; R&D Systems) for 4 h at 37° C. Cells were plated at 0.1×10^6 per well and cultured in a humidified incubator (5% CO_2, 37°C) for 72 h, harvested, and stained with viability dye

(Fixable Viability Stain 450; BD Biosciences). Programmed death 1 expression on anti-CD3–treated T cells, but not on resting cells, confirmed the activated status of these cells (data not shown). Resting and activated T cells were incubated for 1 h at room temperature with ILDR2-hFc or control Ig (human IgG1; Synagis) at 100 μg/ml in FACS buffer (0.5% BSA, 2 mM EDTA, 0.05% NaN_3 in PBS), and ILDR2-hFc binding was detected using PE-conjugated anti–human IgG (Jackson ImmunoResearch). Cells were washed three times, gated for singlets (forward scatter [FSC]-H versus FSC-A) and for live cells, and ILDR2-hFc binding was determined within this gated population. Data acquisition was performed with MACSQuant Analyzer 10 (Miltenyi Biotec) and analyzed using FlowJo software (v10).

Binding of ILDR2-mFc to mouse CD4 T cells

Untouched $CD4^+CD25^-$ T cells were isolated from pools of spleens of BALB/c mice, using a T cell isolation kit (Miltenyi Biotec), according to the manufacturer's instructions. Following isolation, cells were left untreated (resting) or were activated using polyclonal activation of T cells, with plate-bound anti-CD3 Ab (clone-145-2C11; BD Pharmingen, coated on 96-well plates, at 2 μg/ml, for 4 h at 37°C) and 2 μg/ml soluble anti-CD28 Ab (clone 37.51; eBioscience). Cells were harvested at different time points after activation (12, 24, and 48 h) and stained with 2 μg/ml anti-CD25 Ab (clone PC61; BioLegend) to evaluate T cell activation. For binding of tested proteins, biotinylated (using a DSB-X Biotin Protein Labeling Kit, D-20655; Molecular Probes) ILDR2-mFc or Ig control (mIgG2a) was used. To prevent binding to Fcγ receptors, the ILDR2-mFc protein used for this analysis carries the N297A mutation, resulting in an aglycosylated Fc domain. Cells were incubated for 30 min at room temperature with biotinylated ILDR2-mFc or control Ig at 60 μg/ml in FACS buffer (0.5% BSA and 2 mM EDTA in PBS), washed, and stained with 0.5 mg/ml streptavidin-PE (Jackson ImmunoResearch) for 30 min at room temperature. Resting or activated $CD4^+$ cells were gated for lymphocytes (FSC-A versus side scatter [SSC]-A), followed by live cells, and then further gated for singlets (FSC-H versus FSC-A). Further gating on CD25 was carried out to focus on the population of activated T cells. Data were acquired with a MACSQuant Analyzer 10 (Miltenyi Biotec) and analyzed using FlowJo software.

CIA mouse model

DBA/1 mice were immunized with type II bovine collagen in CFA. No further collagen boost was used in this model. The following proteins were used: ILDR2-mFc, mIgG2a as isotype control (BE0085; Bio X Cell), and the ECD of human TNFR fused to human IgG1 Fc (TNFR-Fc; Enbrel, etanercept; Wyeth Pharmaceuticals). The tested proteins were administered i.p. (100 μg per mouse) from the day of disease onset (day 1) for each mouse individually, followed by three times a week until day 10 after disease onset (total of four administrations). Arthritis severity was assessed using the following clinical scoring system: 0 = normal, 1 = slight swelling and/or erythema, 2 = pronounced edematous swelling, and 3 = joint rigidity. Each limb was graded, thus allowing a maximum score of 12 per mouse. The animals were sacrificed at day 10 postonset of disease. Statistical analysis was carried out using two-way ANOVA with repeated measures for all groups, followed by two-way ANOVA with repeated measures for each test group versus control mIgG2a.

Analysis of anti-collagen Abs in serum

Serum was obtained from blood collected from treated mice at study termination, day 10 postdisease onset, by cardiac puncture. Serum was analyzed for anti-collagen mouse IgG1 (catalog number 559626; clone X56) and mIgG2a (clone R19-15, catalog number 553391; both from BD Pharmingen) by ELISA using plates that were precoated with 50 μl of type II bovine collagen, diluted to 5 μg/ml in Tris-HCl, overnight at 4°C. Because of the large variability in anti-collagen Ig levels, each sample was serially diluted so that comparisons between samples are made on the linear portion of the titration curve. Each sample was then normalized to control serum from arthritic mice.

Autologous cocultures of cytokine-activated T cells and MΦs from healthy donors or RA patients

Monocytes and $CD4^+$ T cells were isolated from healthy donors' or RA patients' blood or buffy coats. T cells were cultured with the following cytokines (obtained from PeproTech) for 6 d to induce cytokine-activated T cells (Tcks): TNF-α (25 ng/ml), IL-6 (100 ng/ml), and IL-15 (100 ng/ml). MΦs were differentiated from monocytes with M-CSF (50 ng/ml; PeproTech) for 6 d. Autologous Tcks and MΦs were cocultured for 24 h in the presence of various concentrations of ILDR2-hFc or control Ig (human IgG1; Synagis). TNF-α secretion was evaluated by ELISA using a Human TNF-α Cytoset (Invitrogen). Additional cytokines and chemokines were evaluated by Luminex, using a human 30-Plex Panel (Thermo Fisher Scientific).

qRT-PCR analysis of normal human tissues

RNA samples from normal human tissues were obtained from different sources (ABS, BioChain, Ambion, Asterand, Genomics Collaborative, Tel Aviv Sourasky Medical Center, and Magen David Adom in Israel Blood Services Center). cDNA was synthesized by reverse transcription (RT) of each total RNA sample, previously treated with DNase I (Ambion), using Random Hexamer primers (Invitrogen), RNasin (Promega) and Multi-Scribe polymerase. qRT-PCR was carried out using these cDNA samples as template in a SYBR Green I assay (Applied Biosystems) with UNG enzyme.

Primers were specific for the short transcript: forward primer spanning the junction of exons 5 and 6: 5′-TGTGGAGATTATGCCAGAGTGG-3′ and reverse primer derived from the intracellular region: 5′-GACATTTCTCTCGATCGCTCTGT-3′. Fluorescence was detected using a PE Applied Biosystems SDS 7000. The cycle in which the reactions achieved a threshold level of fluorescence (Ct = threshold cycle) was registered and was used to calculate the relative transcript quantity (Q) in the RT reactions, using the equation $Q = \text{efficiency}^{-Ct}$. The efficiency of the PCR reaction was calculated from a standard curve, created by using serial dilutions of several RT reactions. To minimize inherent differences in the RT reactions, the resulting relative quantities were normalized using a normalization factor calculated by assessing the relative quantity (Q, as described above) for several HSKPs in each cDNA sample and dividing by the median quantity of this gene in all panel samples to obtain the "Relative Q rel to MED." Then, for each sample, the median of the relative Q rel to MED of the selected HSKPs was calculated and served as the normalization factor of this sample for further calculations. For each RT sample, the expression of the

specific amplicon was normalized to the normalization factor calculated from the expression of different HSKPs. The HSKPs that were used for the calibration of the “normal panel” were HPRT1, SDHA, and G6PD.

Evaluation of murine T cell apoptosis

$CD4^+CD25^-$ murine T cells were stimulated with plate-bound anti-CD3 (2 μg/ml) alone or in the presence of 10 μg/ml ILDR2-mFc or control Ig (mIgG2a). Live gated and ungated CD4 T cells were analyzed by FACS at 24 and 48 h poststimulation for the cell death marker 7-aminoactinomycin D and for the expression of the early apoptosis marker annexin V, using an PE Annexin V Apoptosis Detection Kit I (BD Biosciences).

Results

Structural analysis of ILDR2

Human ILDR2 mRNA (GenBank accession: NM_199351, https://www.ncbi.nlm.nih.gov/nuccore/NM_199351) encodes a 639-aa type I membrane protein containing a signal peptide at its N terminus, followed by a large V-type Ig (IgV) domain of 148 aa, a stalk region of 19 aa, a transmembrane domain of 20 aa, and an intracellular tail of 433 aa (Fig. 1A). This protein shows 94% overall homology to its murine ortholog, Ildr2 (GenBank accession: NM_001164528, https://www.ncbi.nlm.nih.gov/nuccore/NM_001164528), with 96% identity and 98% similarity in the ECD. Alignment of the protein sequences of ILDR2 and its two paralogs reveals overall homology of 39 and 44% to ILDR1 and LSR, respectively. There is 36% identity and 52% similarity between the ECDs of ILDR2 and ILDR1 and 47% identity and 66% similarity between the ECDs of ILDR2 and LSR (Fig. 1B). A stretch of amino acids enriched in cysteine and proline residues (cysteine and proline [CCP]-rich domain) is located at the juxtamembrane region of the intracellular domain of human and mouse ILDR2 (Fig. 1A). This CCP-rich domain is also found in the two other paralogs: ILDR1 and LSR (Fig. 1B).

The structure of the human *ILDR2* gene is depicted in Fig. 1C. Shown are the splice variants of ILDR2, with the longest transcript (comprising 10 coding exons) encoding the membrane protein described above and presented in Fig. 1A. A novel shorter isoform, revealed by Compugen’s LEADS platform (15), encodes a type I membrane protein with the same ECD but a significantly shorter and distinct intracellular tail of 48 aa. Both the long and short isoforms contain the CCP-rich domain. A third splice variant predicted by LEADS encodes a protein lacking the transmembrane domain and, thus, is expected to be a secreted isoform. In addition, RT-PCR analysis revealed another transcription variant, in which the fourth exon (an exon of 57 bp that codes for the 19-aa stalk region) is spliced out. This variant contains the transmembrane domain but has a shorter ECD without the stalk region. A similar alternative exon of 57 bp coding for the stalk region appears in LSR (7). Interestingly, an exon of 57 bp, which codes for the stalk region, is also present in the gene coding for VISTA, another B7-like protein (30).

Splice isoforms of the mouse *Ildr2* gene have been described. Four mouse isoforms were reported by Dokmanovic-Chouinard et al. (9), and three of them have the same structure as

the human long isoform, soluble isoform, and Skip 4 variant depicted in Fig. 1B. Seven mouse splice isoforms were later described by Higashi et al. (7), two of which have the same structure as the human long and soluble isoforms shown in Fig. 1C. In that study, the Skip 4 variant murine version was also detected but in the context of the long isoform (exons 1, 2, 3, 5–10), whereas the human Skip 4 variant that we identified was in the context of the short isoform (exons 1, 2, 3, 5–5′).

Aligning the sequence of ILDR2 to the National Center for Biotechnology Information Reference Sequences (RefSeq) record of non-redundant proteins (https://www.ncbi.nlm.nih.gov/refseq/about/nonredundantproteins/) using the Basic Local Alignment Search Tool revealed low sequence homology to other B7-like proteins. Pair alignments between ILDR2 and these proteins show various similar signatures along the IgV domain. This domain was found to mediate the interaction of B7-like ligands with their counterpart receptors on T cells, as shown, for example, in the case of CD80 and CD86 (see PDB 1I85 and PDB 1I8L) (31, 32). The sequence identity and similarity between ILDR2 IgV and that of other B7-like proteins ranges between 15 and 21% and between 24 and 36%, respectively (Table I). This degree of homology is similar to that exhibited among other members of the B7 family (33).

Multiple sequence alignment between the IgV domains of ILDR2 and that of other B7-like proteins (Fig. 1D) reveals shared canonical cysteine residues and the DxGxYxC motif. In addition, a unique long helical loop containing two noncanonical cysteines is evident between the C and C′ strands of the ILDR2 IgV structure (Fig. 1D, 1E). The two ILDR2 paralogs, LSR and ILDR1, also have an extended loop with two noncanonical cysteines between the C and C′ strands.

Expression of ILDR2 in human and mouse tissues

Information on expression of human *ILDR2* mRNA was extracted from the Genotype-Tissue Expression (GTEx) database (34). The results presented in Fig. 2A indicate high expression in testis and high to moderate expression in brain. Lower expression is observed in other tissues, such as kidney, heart, and colon. qRT-PCR analysis using primers specific to the short ILDR2 transcript on RNA samples from various human normal tissues (Supplemental Fig. 1) also showed highest expression in brain and testis, moderate expression in kidney, PBMCs, and stomach, and low expression in various other tissues. Support for the expression of ILDR2 protein was obtained by querying the Proteomics Database (https://www.proteomicsdb.org/proteomicsdb/#overview) and the Human Proteome Map (http://www.humanproteomemap.org/query.php) of protein mass spectrometry data; peptides derived from ILDR2 were identified in testis, brain frontal cortex, and retina.

The relative expression pattern of murine *Ildr2* mRNA was extracted from the data available at the GNF Gene Expression Atlas (35). The results point to a roughly similar expression pattern as that described above for human *ILDR2* mRNA, indicating high to moderate expression in various regions within the brain (Fig. 2B). High to moderate expression was also observed in different structures in the eye (retina, iris, eye cup, lens, ciliary bodies), which are not part of the data available at GTEx for human RNA expression. Moderate expression also appears in kidney, and no or significantly lower expression occurs in other

tissues. Unlike the high *ILDR2* mRNA expression observed in human testis, no murine *Ildr2* mRNA was detected in mouse testis.

Expression of ILDR2 on immune cells

Expression of the ILDR2 protein on inflamed samples obtained from IBD patients (ulcerative colitis and Crohn's disease) was evaluated by IHC analysis using an anti-ILDR2 polyclonal Ab. Results point to increased ILDR2 expression in reactive epithelium and immune cells in IBD samples compared with normal colon and small intestine (Fig. 3).

We further evaluated the expression of ILDR2 on immune cells by FACS analysis using an anti-ILDR2 mAb. Human PBMCs were gated to lymphocytes and monocytes and stained for immune markers (Fig. 4A) to identify immune cell subtypes. Further staining with anti-ILDR2 Ab (shown in Fig. 4B) indicated ILDR2 expression on the three monocyte subtypes, identified based on their relative expression of CD14 and CD16 [reviewed in Wong et al. (36)]. The highest ILDR2 expression was observed in the $CD16^+$ monocyte subsets (i.e., $CD14^+$ $CD16^+$ "intermediate monocytes" and $CD14^{low}$ $CD16^+$ "nonclassical monocytes"). Weak staining for ILDR2 was also observed on $CD56^+$ lymphocytes (mostly NK and NKT cells). The other immune cell subsets tested did not show significant or consistent staining.

ILDR2 protein expression was upregulated on human monocyte–derived MΦs (Fig. 4C). In agreement, RT-PCR analysis indicated that the expression of *ILDR2* mRNA was higher in monocyte-derived MΦs compared with monocytes (Fig. 4D), suggesting that ILDR2 is upregulated following differentiation of human monocytes into MΦs by M-CSF.

ILDR2 inhibits T cell activation

The functional effect of the ILDR2 protein on T cell activation was tested following ectopic expression of the full ILDR2 protein in stimulator cells. These are Bw5147 cells (a murine thymoma cell line) engineered to express membrane-bound anti-human CD3 single-chain Ab fragments (25). The long and short isoforms of ILDR2, which have the same ECD, were tested. Stimulator cells expressing the known costimulator ICOSL served as positive control for positive costimulation, whereas cells expressing the coinhibitory ligand PD-L1 served as positive control for coinhibition. Expression of the long or short isoforms of ILDR2 on stimulator cells exerted an inhibitory effect on bulk (CD3) human T cell activation, and an inhibitory effect was also observed when the well-established coinhibitory ligand PD-L1 was expressed on these cells (Fig. 5A). The stronger T cell inhibitory effect observed with cells expressing the short isoform might stem from an ~10-fold higher surface expression of this isoform compared with the long isoform on stimulator cells (data not shown). Using the same experimental system, we show that ILDR2 expressed on stimulator cells also inhibited activation of isolated human CD8 T cells (Supplemental Fig. 2A).

To further examine the immunomodulatory role of ILDR2 on human and mouse T cell responses, we used ILDR2-Fc (ILDR2-hFc or ILDR2-mFc).

A clear dose-dependent reduction in T cell proliferation by soluble ILDR2-hFc was observed when human $CD4^+$ T cells were activated with anti-CD3 and anti-CD28 in the presence of irradiated autologous PBMCs (Fig. 5B). Similarly, plate-bound ILDR2-hFc

inhibited proliferation of human CD4 and CD8 T cells in the presence of coimmobilized anti-CD3 and soluble anti-CD28 (Supplemental Fig. 2B). A pronounced inhibitory effect of ILDR2-hFc was also evident using human T cell blasts, following their reactivation with anti-CD3 (Fig. 5C). The inhibition displayed by ILDR2-hFc was substantially stronger than that observed with PD-L1–Fc, used as positive control (ED_{50} = 0.54 and 1.3 μg/ml, respectively).

Similar results were obtained with mouse T cells activated with anti-CD3/CD28-coated beads. Upon coimmobilization on beads, ILDR2-mFc suppressed murine $CD4^+$ T cell activation, manifested as a reduction in T cell proliferation, in the two mouse strains tested (SJL and BALB/C, Fig. 5D). ILDR2-mFc in soluble form also displayed pronounced and dose-dependent inhibition of Ag-specific T cell activation, following $OVA_{323–339}$-induced activation of $CD4^+$ T cells from DO11.1 ($OVA_{323–339}$-TCR transgenic) mice in the presence of syngeneic irradiated APCs (Fig. 5E).

The inhibitory effect of ILDR2-Fc on human or murine T cell activation was also evident when additional readouts were used, including cytokine secretion and expression of T cell activation markers (data not shown).

Of note, ILDR2-Fc present in a soluble form did not exert inhibitory effects on purified T cells (data not shown). Such effects were displayed only upon immobilization of ILDR2-Fc on beads or plates or when APCs were also present in the T cell assays. This observation implies a requirement for cross-linking of ILDR2-Fc to a surface, such as beads, or onto APCs via their Fcγ receptors. Further support for this notion was obtained from experiments using a N297A Fc mutated variant of ILDR2-mFc, resulting in an aglycosylated Fc domain with greatly reduced ability to bind Fcγ receptors. This variant showed inhibitory activity upon its cross-linking to beads or plates, but no such activity was displayed when it was tested in a soluble form in the presence of APCs (Supplemental Fig. 3, data not shown).

To assess whether induction of T cell apoptosis contributes to the inhibitory effect of ILDR2-Fc on T cell proliferation, we evaluated the levels of annexin V (marker of apoptosis) and 7-aminoactinomycin D (cell death marker). The results indicate that the levels of early and late apoptosis were not enhanced; rather, they were somewhat reduced in the presence of ILDR2-Fc (Supplemental Fig. 4), implying that apoptosis does not underlie the inhibitory effect of ILDR2-Fc on T cell responses.

ILDR2-Fc binds activated T cells

Based on the robust inhibitory activity observed for ILDR2 on T cells, we asked whether T cells express a putative counterpart for ILDR2 and tested the binding of ILDR2-Fc to resting or activated T cells. The results show binding of ILDR2-Fc to human or mouse activated T cells but no detectable binding to resting nonactivated T cells (Fig. 6). Binding of ILDR2-hFc was detectable on $CD4^+$ or $CD8^+$ activated human T cells (Fig. 6A, 6B, respectively). The kinetics of such binding was tested using ILDR2-mFc and mouse $CD4^+$ T cells and indicates weak binding, which was already evident by 12 h post cell activation (Fig. 6C). Similar binding kinetics was observed using activated human $CD4^+$ T cells (data not shown).

These findings suggest inducible expression of a counterpart receptor for ILDR2 following T cell activation.

ILDR2-Fc displays beneficial effects in the CIA model of RA

The robust inhibitory effect on T cell activation displayed by the ILDR2-Fc protein in various in vitro experimental systems prompted us to test its effect in vivo, using the CIA mouse model of RA, in which effector T cells have been shown to play a critical role in the induction and maintenance of inflammatory joint disease (37). Therapeutic administration of ILDR2-mFc showed a clear trend toward a reduction in clinical score, although this did not reach statistical significance ($p = 0.079$ versus PBS) (Fig. 7A). We also analyzed the serum levels of murine IgG1 and IgG2a Abs to type II collagen. IgG subclass expression is influenced by multiple factors, including the prevailing cytokine environment. Isotype switching to IgG2a or IgG1 is induced by Th1 or Th2 cytokines, respectively. Thus, these isotypes are valuable in vivo indicators of Th1 and Th2 responses. The results indicate a statistically significant increase in the IgG1/IgG2a ratio in mice treated with ILDR2-mFc ($p = 0.041$ versus PBS) (Fig. 7B). These results point to a Th1 to Th2 shift taking place following in vivo ILDR2-mFc treatment and are evidence of an immunomodulatory effect toward a less pathogenic immune response (i.e., a shift from proinflammatory Th1 to anti-inflammatory Th2) and restoration of immune homeostasis.

Inhibitory effect of ILDR2-Fc in a translational assay mimicking interactions of T cells and MΦs in the RA synovium

The therapeutic potential of ILDR2-Fc for treatment of RA was further studied using cocultures of Tcks and MΦs from healthy donors and from RA patients. Such cocultures have been suggested to mimic the deleterious interaction of these cells in the RA synovium, which drive the secretion of proinflammatory cytokines (in particular TNF-α) and play a major role in the pathology of RA. This experimental system provides a translational tool to evaluate potential therapies for RA (38).

As shown in Fig. 8A, addition of ILDR2-hFc to these synovial-like cocultures induced a dose-dependent inhibition in TNF-α secretion. ILDR2-hFc downregulated additional proinflammatory and regulatory cytokines and chemokines in these cultures, with pronounced inhibitory effects on CCL3, CCL5, GM-CSF, IL-12, IFN-γ, IL-1RA, IL-5, and IL-6 (Fig. 8C). Mild inhibition was observed for secretion of IL-17, IL-13, and soluble IL-2R, whereas the production of IL-10, IL-15, IFN-α, and IL-7 was not affected (data not shown). ILDR2-hFc also inhibited the secretion of TNF-α in such cocultures from RA patients (Fig. 8B), demonstrating that the ILDR2 pathway is functional and responsive in these patients. Binding of ILDR2-hFc to Tcks suggests upregulation of the putative ILDR2 receptor in these cells to a similar extent as that observed with anti-CD3–or anti-CD3/CD28–activated T cells (data not shown).

Discussion

This article presents ILDR2 as a novel member of the B7-like family of immunomodulators. Taken together, our data show that ILDR2 exerts robust inhibitory effects on human and

mouse T cells when tested as an Fc fusion protein (ILDR2-Fc) or upon overexpression of the full membrane protein. Similar to other B7-like negative regulators [e.g., B7-H4 (39) and VISTA (30)], ILDR2 negatively regulates T cell responses by suppressing early TCR activation and cell division but without enhancing apoptosis. The robust inhibition of T cell activation exerted by ILDR2 is most likely due to its agonistic activity on an inhibitory receptor, rather than inhibition of a T cell–stimulatory pathway. Two key observations support this notion: the ability of ILDR2-Fc to inhibit activation of purified T cells (i.e., in the absence of APCs or other ILDR2-expressing cells) and the need to cross-link ILDR2-Fc (to beads, plates, or to Fcγ receptors) for it to exert its inhibitory activity.

Although the counterpart receptor of ILDR2 has not been identified, the binding studies presented in this article indicate expression of an inducible counterpart for ILDR2 on activated T cells, which can be detected during early TCR activation. This observation is reminiscent of other negative receptors of the B7-like family that are upregulated on T cells following activation, such as CTLA4, programmed death 1 (PD-1), and T cell immunoreceptor with Ig and ITIM domains (TIGIT). Furthermore, the higher expression observed for ILDR2 in immune-privileged tissues, such as brain, eye, and testis, is reminiscent of the expression pattern observed for other negative immunomodulators of the B7/CD28 family, including PD-L1, which are part of the mechanisms of immune tolerance induction operating in immune-privileged sites (40, 41).

We describe the protein structure of ILDR2 and its two paralogs, ILDR1 and LSR (ILDR3), and demonstrate that, although these proteins show similarities to those of known B7-like family members, they share unique structural features, such as the presence of a CCP-rich domain located at the juxtamembrane region of the intracellular domain and a unique extended loop with noncanonical cysteine residues in the IgV within their ECDs.

ILDR2 and its two paralogs, ILDR1 and LSR, have been identified as protein components of tTJs, specialized structures where the corners of three epithelial cells meet that are required for full barrier function of the cellular sheet (8); thus, they function as a type of cell adhesion molecule. Members of the IgSF account for a large proportion of cell adhesion molecules (42). Some IgSF proteins that have properties of adhesion molecules have also been shown to perform important immunological functions, including immune checkpoint regulators. For example, poliovirus receptor (PVR)/CD155 belongs to the family of nectin-like adhesion proteins and is a ligand of TIGIT (also designated as Washington University adhesion molecule), a known immune checkpoint in NK cells and T cells. The PVR–TIGIT interaction plays dual roles in cell adhesion and cell signaling (43), including adhesion of T follicular helper cells to follicular DCs (44). Another example in this family is PVRL2/CD112/Nectin-2, a member of the nectin family of adhesion molecules, which is a ligand of CD226 (a prominent costimulatory receptor in the TIGIT pathway) and of a novel checkpoint CD112R/PVR Ig (45). Recently, another adhesion molecule, PSGL-1, was characterized as a novel negative regulator of T cell function that is upregulated in activated T cells (46). Similar to these IgSF proteins, ILDR2 seems to play dual roles, as a tTJ component and as a novel immunomodulator (presented in this article).

In this article, we also present the therapeutic effect of ILDR2-mFc in CIA, a mouse model of RA. In addition to its beneficial effect on disease score, administration of ILDR2-mFc led to an increase in the IgG1/IgG2a ratio, pointing to a shift from proinflammatory Th1 responses to anti-inflammatory Th2 responses. The ILDR2-Fc–mediated immunomodulatory Th1/Th2 shift is supported by additional in vitro and in vivo findings reported by Podojil et al. (47). Of relevance is the strong upregulation of *ILDR2* mRNA upon polarization of human DCs to DC2 cells (14), which promotes the differentiation of Th2 cells.

To further substantiate the immunomodulatory activity of ILDR2-Fc in the context of RA, we used a translational assay that mimics the deleterious interaction of immune cells in the RA synovium. In this assay, ILDR2-hFc decreased the secretion of TNF-α and other proinflammatory cytokines and chemokines that play a major role in the pathology of RA. These findings further demonstrate the immunomodulatory activity of ILDR2-Fc and its potential to affect autoimmune processes and inflammation in patients.

The therapeutic efficacy and mode of action of ILDR2-Fc were further characterized using additional models of autoimmune diseases and a translational assay, focusing primarily on multiple sclerosis and its mouse model, EAE, as reported by Podojil et al. (47). The results point to ILDR2-Fc as a promising novel therapeutic agent that displays a unique mode of action, combining immunomodulation and regulation of immune homeostasis, as well as regulatory T cell induction and re-establishment of Ag-specific immune tolerance, leading to durable amelioration of autoimmunity.

To summarize, ILDR2 is a novel negative regulator of T cell responses, with potential roles in the modulation of immune responses, as well as critical implications for the development of autoimmunity and other diseases, such as cancer.

Supplementary Material

Refer to Web version on PubMed Central for supplementary material.

Acknowledgments

We thank Ami Tamir and Elisheva Yonish-Rouach for critical support in protein production, Ofer Levy for providing input on discovery and expression aspects, Yossef Kliger for critical assistance in manuscript preparation, and Drew M. Pardoll for critical review of the manuscript.

Abbreviations used in this article:

CCP	cysteine and proline
CIA	collagen-induced arthritis
DC	dendritic cell
ECD	extracellular domain
FSC	forward scatter

GTex	Genotype-Tissue Expression
HSKP	housekeeping gene
IBD	inflammatory bowel disease
IgSF	Ig superfamily
IgV	V-type Ig domain
IHC	immunohistochemistry
ILDR	Ig-like domain–containing receptor
ILDR-Fc	a fusion protein of ILDR2 extracellular domain with an Fc fragment
ILDR2-hFc	ECD of human ILDR2 (aa 1–184) fused to the Fc region (C and hinge regions) of human IgG1
ILDR2-mFc	ECD of human ILDR2 (aa 1–184) fused to the Fc region (C and hinge regions) of mouse IgG2a
LSR	lipolysis-stimulated receptor
MΦ	macrophage
mIgG2a	mouse IgG2a
PD-L1	programmed death ligand 1
PVR	poliovirus receptor
qRT-PCR	quantitative RT-PCR
RA	rheumatoid arthritis
RT	reverse transcription
SSC	side scatter
Tck	cytokine-activated T cell
TIGIT	T cell immunoreceptor with Ig and ITIM domains
TNFR-Fc	ECD of human TNFR fused to human IgG1 Fc
tTJ	tricellular tight junction
VISTA	V-domain Ig suppressor of T cell activation

References

1. Zhang Q, and Vignali DA. 2016 Co-stimulatory and co-inhibitory pathways in autoimmunity. Immunity 44: 1034–1051. [PubMed: 27192568]
2. Chen L, and Flies DB. 2013 Molecular mechanisms of T cell co-stimulation and co-inhibition. Nat. Rev. Immunol 13: 227–242. [PubMed: 23470321]

3. Ceeraz S, Nowak EC, and Noelle RJ. 2013 B7 family checkpoint regulators in immune regulation and disease. Trends Immunol. 34: 556–563. [PubMed: 23954143]
4. Yao S, Zhu Y, and Chen L. 2013 Advances in targeting cell surface signalling molecules for immune modulation. Nat. Rev. Drug Discov 12: 130–146. [PubMed: 23370250]
5. Leitner J, Grabmeier-Pfistershammer K, and Steinberger P. 2010 Receptors and ligands implicated in human T cell costimulatory processes. Immunol. Lett 128: 89–97. [PubMed: 19941899]
6. Ohtani H, Nakajima T, Akari H, Ishida T, and Kimura A. 2011 Molecular evolution of immunoglobulin superfamily genes in primates. Immunogenetics 63: 417–428. [PubMed: 21390552]
7. Higashi T, Tokuda S, Kitajiri S, Masuda S, Nakamura H, Oda Y, and Furuse M. 2013 Analysis of the 'angulin' proteins LSR, ILDR1 and ILDR2–tricellulin recruitment, epithelial barrier function and implication in deafness pathogenesis. J. Cell Sci 126: 966–977. [PubMed: 23239027]
8. Ikenouchi J, Furuse M, Furuse K, Sasaki H, Tsukita S, and Tsukita S. 2005 Tricellulin constitutes a novel barrier at tricellular contacts of epithelial cells. J. Cell Biol 171: 939–945. [PubMed: 16365161]
9. Dokmanovic-Chouinard M, Chung WK, Chevre JC, Watson E, Yonan J, Wiegand B, Bromberg Y, Wakae N, Wright CV, Overton J, et al. 2008 Positional cloning of "Lisch-Like," a candidate modifier of susceptibility to type 2 diabetes in mice. PLoS Genet. 4: e1000137. [PubMed: 18654634]
10. Yen FT, Roitel O, Bonnard L, Notet V, Pratte D, Stenger C, Magueur E, and Bihain BE. 2008 Lipolysis stimulated lipoprotein receptor: a novel molecular link between hyperlipidemia, weight gain, and atherosclerosis in mice. J. Biol. Chem 283: 25650–25659. [PubMed: 18644789]
11. Watanabe K, Watson E, Cremona ML, Millings EJ, Lefkowitch JH, Fischer SG, LeDuc CA, and Leibel RL. 2013 ILDR2: an endoplasmic reticulum resident molecule mediating hepatic lipid homeostasis. PLoS One 8: e67234. [PubMed: 23826244]
12. Chandra R, Wang Y, Shahid RA, Vigna SR, Freedman NJ, and Liddle RA. 2013 Immunoglobulin-like domain containing receptor 1 mediates fat-stimulated cholecystokinin secretion. J. Clin. Invest 123: 3343–3352. [PubMed: 23863714]
13. Reaves DK, Fagan-Solis KD, Dunphy K, Oliver SD, Scott DW, and Fleming JM. 2014 The role of lipolysis stimulated lipoprotein receptor in breast cancer and directing breast cancer cell behavior. PLoS One 9: e91747. [PubMed: 24637461]
14. Gueguen C, Bouley J, Moussu H, Luce S, Duchateau M, Chamot-Rooke J, Pallardy M, Lombardi V, Nony E, Baron-Bodo V, et al. 2016 Changes in markers associated with dendritic cells driving the differentiation of either TH2 cells or regulatory T cells correlate with clinical benefit during allergen immunotherapy. J. Allergy Clin. Immunol 137: 545–558. [PubMed: 26522402]
15. Sorek R, Ast G, and Graur D. 2002 Alu-containing exons are alternatively spliced. Genome Res. 12: 1060–1067. [PubMed: 12097342]
16. Krogh A, Larsson B, von Heijne G, and Sonnhammer EL. 2001 Predicting transmembrane protein topology with a hidden Markov model: application to complete genomes. J. Mol. Biol 305: 567–580. [PubMed: 11152613]
17. Petersen TN, Brunak S, von Heijne G, and Nielsen H. 2011 SignalP 4.0: discriminating signal peptides from transmembrane regions. Nat. Methods 8: 785–786. [PubMed: 21959131]
18. Zdobnov EM, and Apweiler R. 2001 InterProScan–an integration platform for the signature-recognition methods in InterPro. Bioinformatics 17: 847–848. [PubMed: 11590104]
19. Jones DT 1999 Protein secondary structure prediction based on position-specific scoring matrices. J. Mol. Biol 292: 195–202. [PubMed: 10493868]
20. Cheng J, Randall AZ, Sweredoski MJ, and Baldi P. 2005 SCRATCH: a protein structure and structural feature prediction server. Nucleic Acids Res. 33 (Web Server): W72–W76. [PubMed: 15980571]
21. Katoh K, Misawa K, Kuma K, and Miyata T. 2002 MAFFT: a novel method for rapid multiple sequence alignment based on fast Fourier transform. Nucleic Acids Res. 30: 3059–3066. [PubMed: 12136088]
22. Rice P, Longden I, and Bleasby A. 2000 EMBOSS: the European molecular biology open software suite. Trends Genet. 16: 276–277. [PubMed: 10827456]

23. Needleman SB, and Wunsch CD. 1970 A general method applicable to the search for similarities in the amino acid sequence of two proteins. J. Mol. Biol. 48: 443–453. [PubMed: 5420325]
24. Boeckmann B, Blatter MC, Famiglietti L, Hinz U, Lane L, Roechert B, and Bairoch A. 2005 Protein variety and functional diversity: Swiss-Prot annotation in its biological context. C. R. Biol 328: 882–899. [PubMed: 16286078]
25. Leitner J, Kuschei W, Grabmeier-Pfistershammer K, Woitek R, Kriehuber E, Majdic O, Zlabinger G, Pickl WF, and Steinberger P. 2010 T cell stimulator cells, an efficient and versatile cellular system to assess the role of costimulatory ligands in the activation of human T cells. J. Immunol. Methods 362: 131–141. [PubMed: 20858499]
26. Pfistershammer K, Klauser C, Pickl WF, Stöckl J, Leitner J, Zlabinger G, Majdic O, and Steinberger P. 2006 No evidence for dualism in function and receptors: PD-L2/B7-DC is an inhibitory regulator of human T cell activation. Eur. J. Immunol 36: 1104–1113. [PubMed: 16598819]
27. Kober J, Leitner J, Klauser C, Woitek R, Majdic O, Stöckl J, Herndler-Brandstetter D, Grubeck-Loebenstein B, Reipert BM, Pickl WF, Pfistershammer K, and Steinberger P. 2008 The capacity of the TNF family members 4-1BBL, OX40L, CD70, GITRL, CD30L and LIGHT to costimulate human T cells. Eur. J. Immunol 38: 2678–2688. [PubMed: 18825741]
28. Leitner J, Klauser C, Pickl WF, Stöckl J, Majdic O, Bardet AF, Kreil DP, Dong C, Yamazaki T, Zlabinger G, et al. 2009 B7-H3 is a potent inhibitor of human T-cell activation: no evidence for B7-H3 and TREML2 interaction. Eur. J. Immunol 39: 1754–1764. [PubMed: 19544488]
29. Pfistershammer K, Majdic O, Stöckl J, Zlabinger G, Kirchberger S, Steinberger P, and Knapp W. 2004 CD63 as an activation-linked T cell co-stimulatory element. J. Immunol 173: 6000–6008. [PubMed: 15528334]
30. Wang L, Rubinstein R, Lines JL, Wasiuk A, Ahonen C, Guo Y, Lu LF, Gondek D, Wang Y, Fava RA, et al. 2011 VISTA, a novel mouse Ig superfamily ligand that negatively regulates T cell responses. J. Exp. Med 208: 577–592. [PubMed: 21383057]
31. Schwartz JC, Zhang X, Fedorov AA, Nathenson SG, and Almo SC. 2001 Structural basis for co-stimulation by the human CTLA-4/B7-2 complex. Nature 410: 604–608. [PubMed: 11279501]
32. Stamper CC, Zhang Y, Tobin JF, Erbe DV, Ikemizu S, Davis SJ, Stahl ML, Seehra J, Somers WS, and Mosyak L. 2001 Crystal structure of the B7-1/CTLA-4 complex that inhibits human immune responses. Nature 410: 608–611. [PubMed: 11279502]
33. Hansen JD, Du Pasquier L, Lefranc MP, Lopez V, Benmansour A, and Boudinot P. 2009 The B7 family of immunoregulatory receptors: a comparative and evolutionary perspective. Mol. Immunol 46: 457–472. [PubMed: 19081138]
34. Lonsdale J, Thomas J, Salvatore M, Phillips R, Lo E, Shad S, Hasz R, Walters G, Garcia F, Young N, et al. 2013 The Genotype-Tissue Expression (GTEx) project. Nat. Genet 45: 580–585. [PubMed: 23715323]
35. Su AI, Wiltshire T, Batalov S, Lapp H, Ching KA, Block D, Zhang J, Soden R, Hayakawa M, Kreiman G, et al. 2004 A gene atlas of the mouse and human protein-encoding transcriptomes. Proc. Natl. Acad. Sci. USA 101: 6062–6067. [PubMed: 15075390]
36. Wong KL, Yeap WH, Tai JJ, Ong SM, Dang TM, and Wong SC. 2012 The three human monocyte subsets: implications for health and disease. Immunol. Res. 53: 41–57. [PubMed: 22430559]
37. Alzabin S, and Williams RO. 2011 Effector T cells in rheumatoid arthritis: lessons from animal models. FEBS Lett. 585: 3649–3659. [PubMed: 21515267]
38. Wenink MH, Santegoets KC, Platt AM, van den Berg WB, van Riel PL, Garside P, Radstake TR, and McInnes IB. 2012 Abatacept modulates proinflammatory macrophage responses upon cytokine-activated T cell and Toll-like receptor ligand stimulation. Ann. Rheum. Dis 71: 80–83. [PubMed: 21908454]
39. Sica GL, Choi IH, Zhu G, Tamada K, Wang SD, Tamura H, Chapoval AI, Flies DB, Bajorath J, and Chen L. 2003 B7-H4, a molecule of the B7 family, negatively regulates T cell immunity. Immunity 18: 849–861. [PubMed: 12818165]
40. Hori J 2008 Mechanisms of immune privilege in the anterior segment of the eye: what we learn from corneal transplantation. J. Ocul. Biol. Dis. Infor 1: 94–100. [PubMed: 20072639]

41. Sugita S, Usui Y, Horie S, Futagami Y, Yamada Y, Ma J, Kezuka T, Hamada H, Usui T, Mochizuki M, and Yamagami S. 2009 Human corneal endothelial cells expressing programmed death-ligand 1 (PD-L1) suppress PD-1 + T helper 1 cells by a contact-dependent mechanism. Invest. Ophthalmol. Vis. Sci 50: 263–272. [PubMed: 18775867]

42. Shimono Y, Rikitake Y, Mandai K, Mori M, and Takai Y. 2012 Immunoglobulin superfamily receptors and adherens junctions. Subcell. Biochem 60: 137–170. [PubMed: 22674071]

43. Stengel KF, Harden-Bowles K, Yu X, Rouge L, Yin J, Comps-Agrar L, Wiesmann C, Bazan JF, Eaton DL, and Grogan JL. 2012 Structure of TIGIT immunoreceptor bound to poliovirus receptor reveals a cell-cell adhesion and signaling mechanism that requires cis-trans receptor clustering. Proc. Natl. Acad. Sci. USA 109: 5399–5404. [PubMed: 22421438]

44. Boles KS, Vermi W, Facchetti F, Fuchs A, Wilson TJ, Diacovo TG, Cella M, and Colonna M. 2009 A novel molecular interaction for the adhesion of follicular CD4 T cells to follicular DC. Eur. J. Immunol 39: 695–703. [PubMed: 19197944]

45. Zhu Y, Paniccia A, Schulick AC, Chen W, Koenig MR, Byers JT, Yao S, Bevers S, and Edil BH. 2016 Identification of CD112R as a novel checkpoint for human T cells. J. Exp. Med 213: 167–176. [PubMed: 26755705]

46. Tinoco R, Carrette F, Barraza ML, Otero DC, Magaña J, Bosenberg MW, Swain SL, and Bradley LM. 2016 PSGL-1 is an immune checkpoint regulator that promotes T cell exhaustion. Immunity 44: 1190–1203. [PubMed: 27192578]

47. Podojil JR, Hecht I, Chiang M-Y, Vaknin I, Barbiro I, Novik A, Neria E, Rotman G, and Miller SD. ILDR2-Fc is a novel regulator of immune homeostasis and inducer of antigen-specific immune tolerance. J. Immunol 200: 2013–2024.

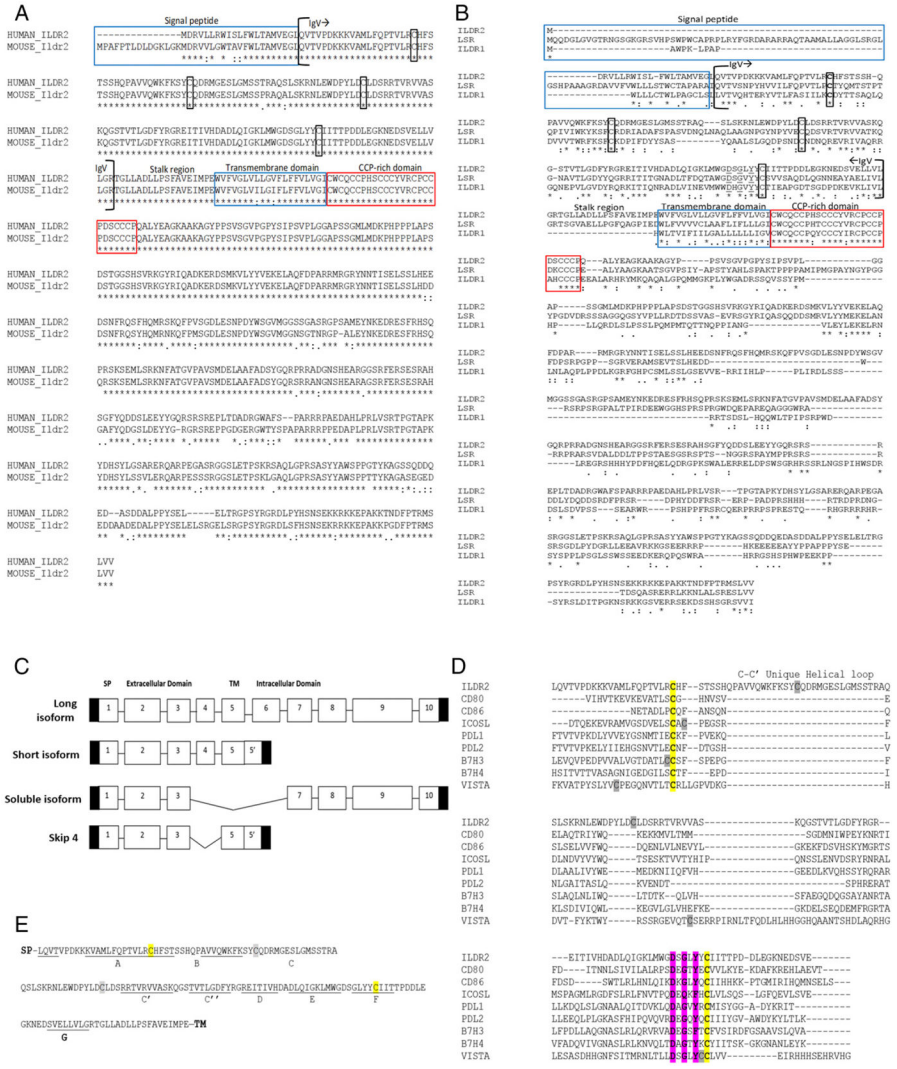

FIGURE 1.

Identification and characterization of ILDR2 as a novel B7-like protein. (**A**) Amino acid sequence alignment and topology of human and mouse ILDR2. The signal peptide and transmembrane domains are outlined in blue rectangles, IgV boundaries are marked by brackets, cysteines are in black rectangles, and the CCP-rich domain is outlined in red. (**B**) Amino acid sequence alignment and topology of human ILDR2, LSR (ILDR3), and ILDR1. Protein domains are marked as described in (A). (**C**) Gene structure and transcription variants of human ILDR2. Shown are exons of alternative spliced transcripts from human ILDR2. The coding regions are depicted as open boxes, and the untranslated regions are represented by black boxes. (**D**) Multiple sequence alignment of the IgV domains of ILDR2 and other proteins of the B7 family. The DxGxYxC motif is highlighted in pink. The canonical cysteine residues in the IgV domain, which are known to form a disulfide bridge, are highlighted in yellow. Noncanonical cysteine residues are highlighted in gray. (**E**) Secondary structure prediction of ILDR2 IgV domain and β-strand organization. Predicted β-strands are marked by the letters A, B, C, C′, C″, D, E, F, and G. IgV canonical cysteines are highlighted in yellow, and noncanonical unique cysteines are highlighted in gray. The

sequence presented spans the entire ECD, from the signal peptide (SP) to the transmembrane domain (TM).

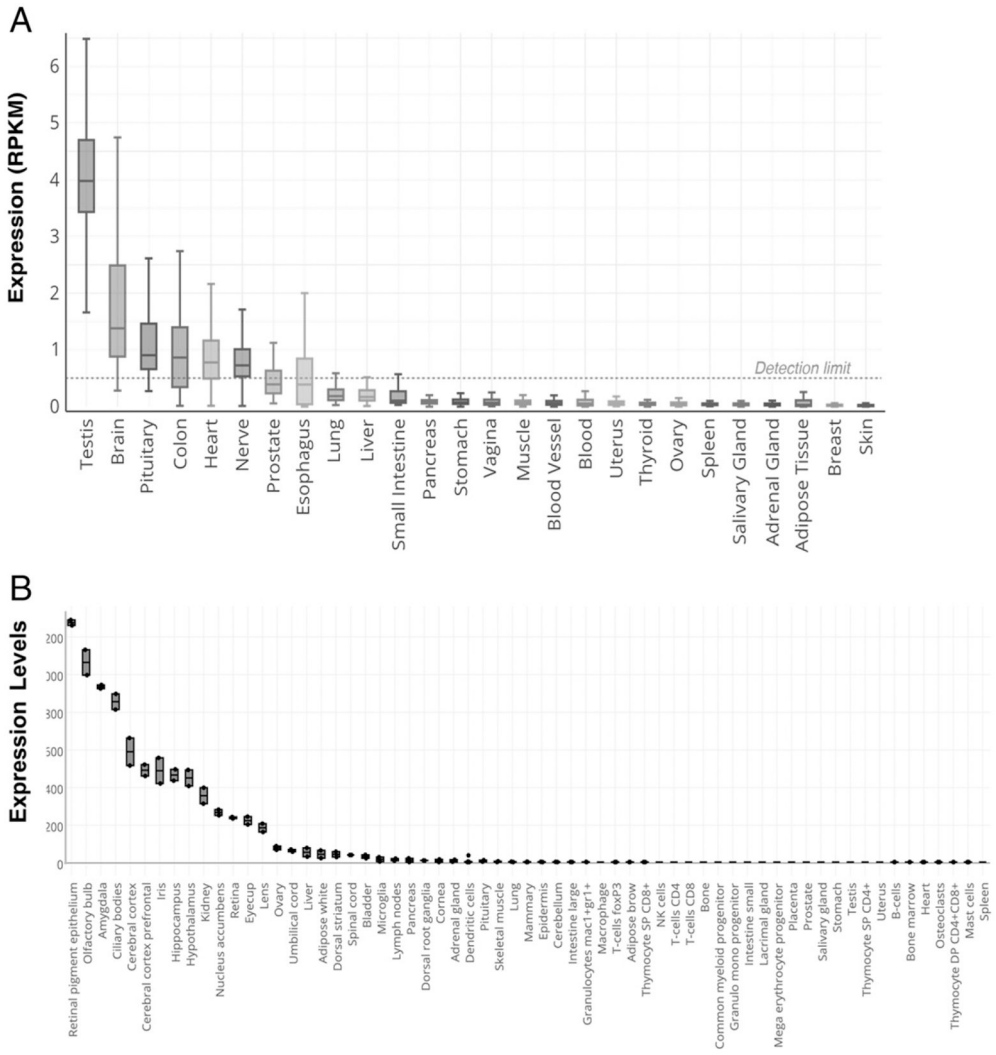

FIGURE 2.

Expression profile of *ILDR2* mRNA. (**A**) *ILDR2* mRNA expression data from normal human tissues were extracted from the GTEx database. The *y*-axis depicts expression levels as reads per kilobase of exon per million fragments mapped (RPKM). (**B**) Expression data of murine *Ildr2* mRNA in normal mouse tissues were extracted from the GNF Gene Expression Atlas. Values shown on the *y*-axis are arbitrary units of microarray gene expression levels.

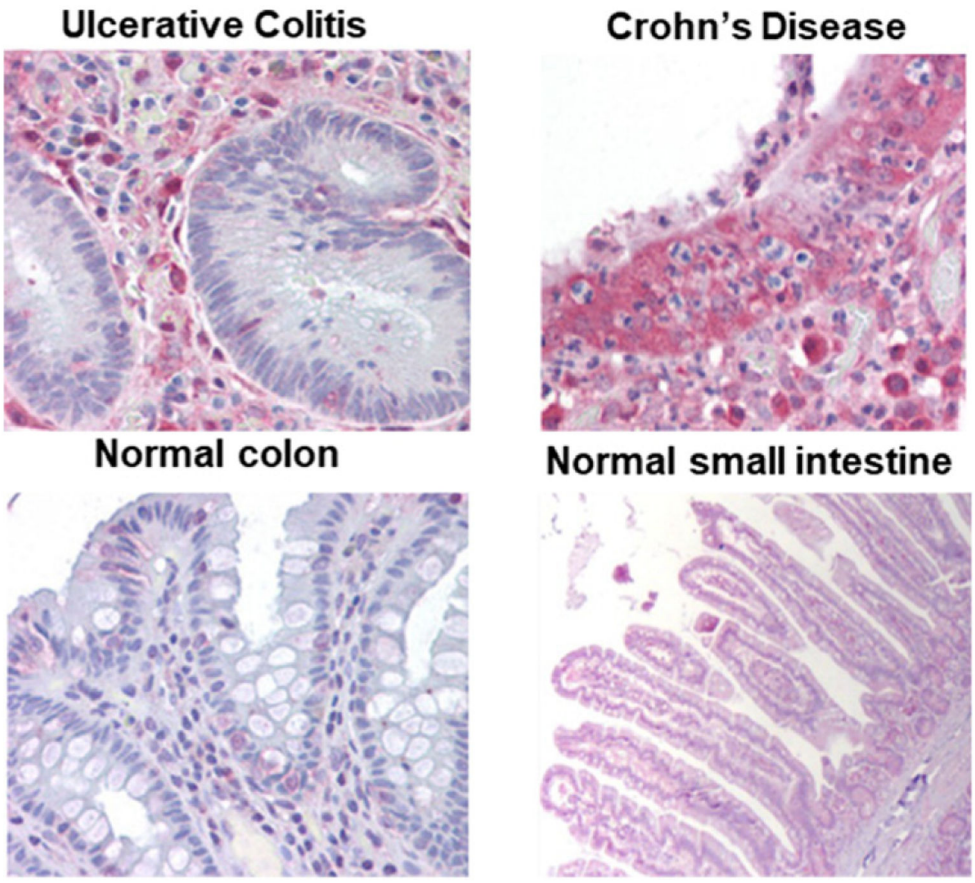

FIGURE 3.

ILDR2 protein expression in inflamed tissues. IHC of ILDR2 expression within inflamed tissue samples of ulcerative colitis and Crohn's disease, as well as normal controls (colon and small intestine), was carried out using anti-ILDR2 polyclonal Ab, Ab-13, as described in Materials and Methods. Shown are representative staining out of two samples for each tissue and condition. Original magnification ×40.

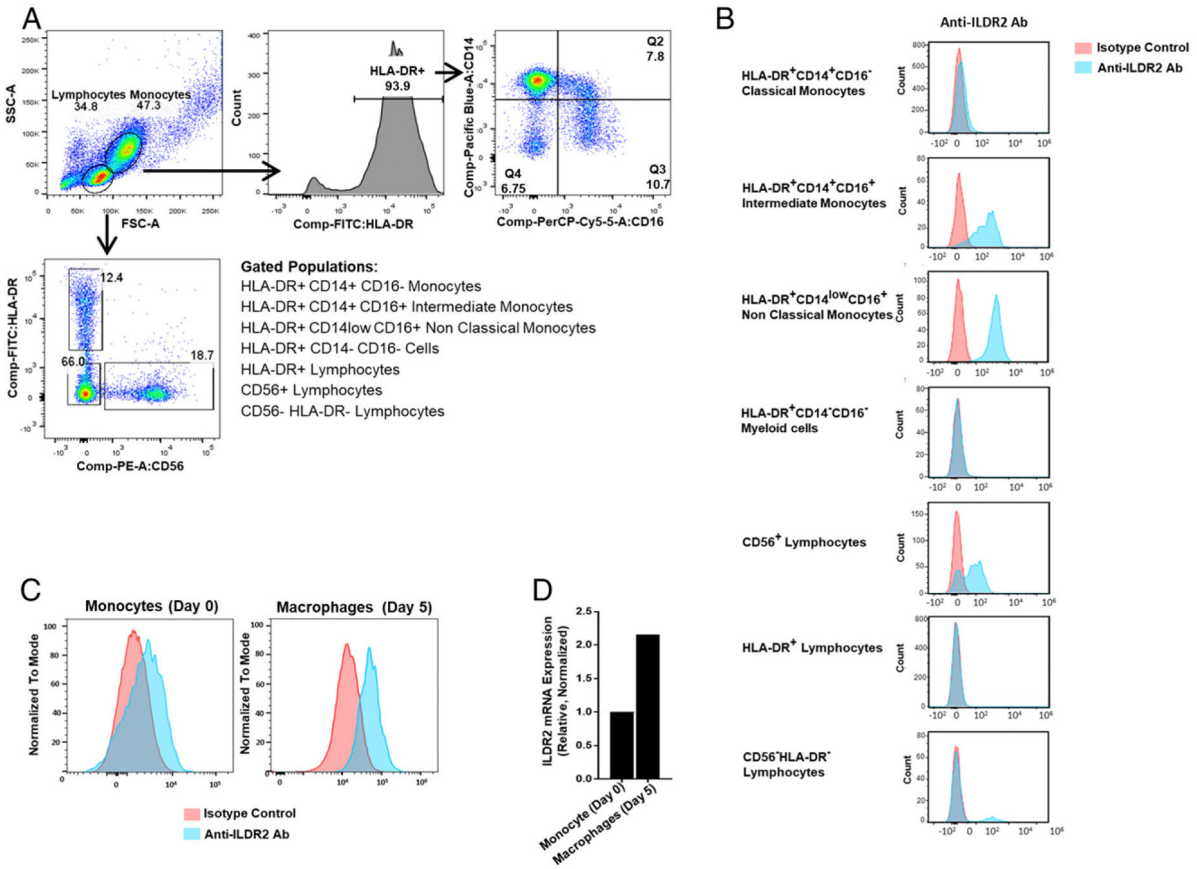

FIGURE 4.

ILDR2 protein expression on immune cell subpopulations. (**A**) Gating strategy for monocyte and lymphocyte subpopulations derived from human PBMCs. Lymphocytes were identified by low FSC/SSC, and monocytes were identified by high FSC/SSC and by HLA-DR$^+$ staining. Monocyte subtypes were defined based on relative expression of CD14 and CD16 (see text for details). HLA-DR$^+$ CD14$^-$ CD16$^-$ cells most likely consist of various other myeloid cells. Lymphocyte populations were defined based on CD56 or HLA-DR expression (CD56$^+$, mostly NK and NKT cells; HLA-DR$^+$, mostly B cells; and CD56$^-$ HLA-DR$^-$, mostly T cells). (**B**) PBMCs from healthy human donors were subjected to FACS analysis and gated as in (A), following staining with Alexa Fluor 647–conjugated anti-ILDR2 Ab (Ab-28) or with isotype control (human IgG1). Shown is one representative healthy donor of seven. (**C** and **D**) ILDR2 expression on human monocyte-derived MΦs. Human MΦs were obtained by in vitro differentiation of blood monocytes using M-CSF, as described in Materials and Methods. (C) ILDR2 protein expression was evaluated on monocytes (day 0) or on monocyte-derived MΦs (day 5, i.e., after incubation of monocytes with M-CSF for 5 d) by FACS analysis using anti-ILDR2 mAb (Ab-28 or isotype control [human IgG1]). Results are shown for one donor and are representative of four donors. (D) *ILDR2* mRNA expression was evaluated by qRT-PCR using RNA derived from the monocytes and monocyte-derived MΦs in (C). Bars show relative ILDR2 expression (normalized to HSKPs) in monocyte-derived macrophages relative to untreated monocytes (i.e., day 0). Results are shown for one donor and are representative of four donors.

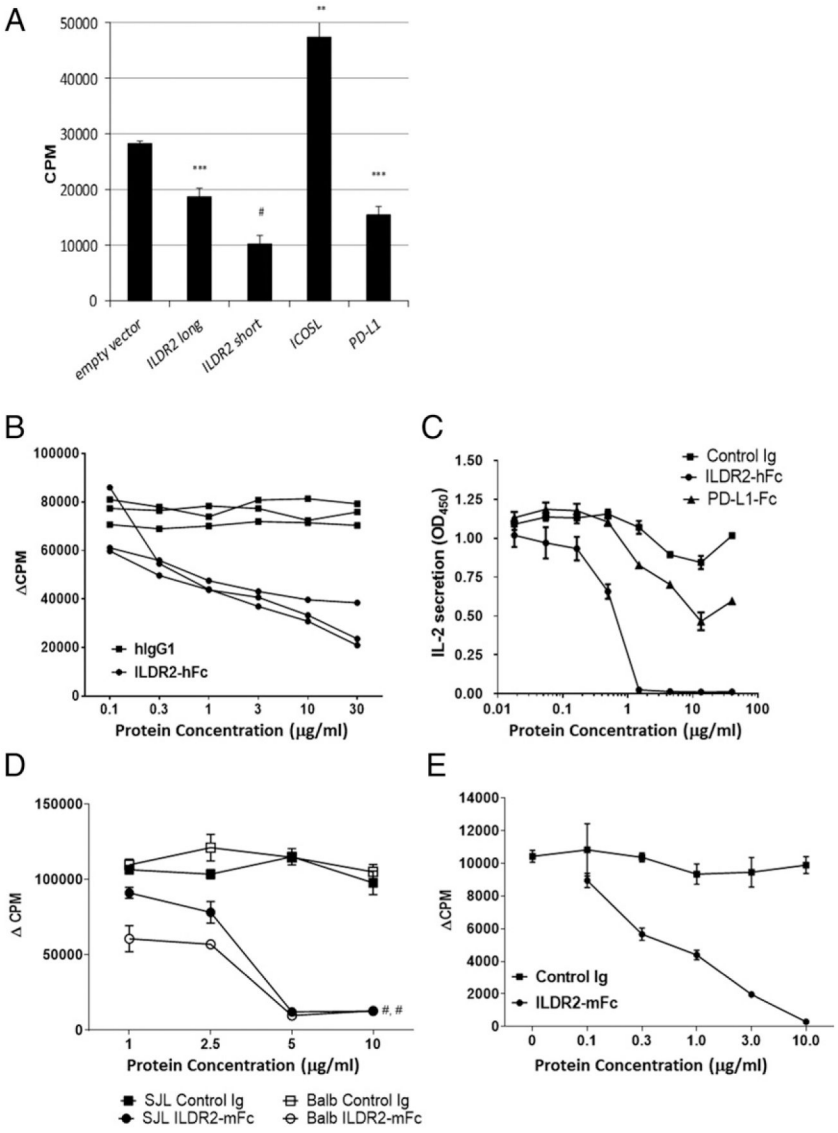

FIGURE 5.

ILDR2 inhibits activation of human and murine T cells. (**A**) Membrane-expressed ILDR2 inhibits human T cell activation. Stimulator cells (a murine thymoma cell line engineered to express membrane-bound anti-human CD3 single-chain Ab fragments) were transfected with expression constructs encoding the long or the short splice variant of human ILDR2. Cells transfected with the empty vector served as negative control. Proliferation of human $CD3^+$ T cells was evaluated upon coculture with stimulator cells expressing the ILDR2 short and long variants, as well as ICOSL or PD-L1, as reference. Shown is a representative experiment of four experiments carried out with a total of three donors. Data are mean ± SEM of triplicate samples. (**B**) Soluble ILDR2-hFc inhibits activation of human T cells. Naive $CD4^+$ T cells obtained from human PBMCs were activated by soluble anti-CD3 and anti-CD28 in the presence of irradiated autologous PBMCs. ILDR2-hFc or isotype control (human IgG1; Synagis) was added at the specified final concentrations. Cell proliferation was evaluated by [^{3}H]thymidine incorporation at 72 h. Shown are representative results

obtained with three human donors. (**C**) Immobilized ILDR2-hFc has an inhibitory effect on reactivation of stimulated human T cells. Human T cell blasts, obtained by stimulation of human PBMCs with PHA and human IL-2 for 10 d, were reactivated for 3 d in 96-well plates coated with anti-CD3, in the presence of ILDR2-hFc or isotype control (recombinant human IgG1-Fc) at the indicated concentrations, as described in *Materials and Methods*. IL-2 secretion was measured by ELISA after 24 h. PD-L1–Fc (recombinant human B7-H1/Fc) was used as positive control. Shown are representative results for one of three experiments. (**D**) Bead-immobilized ILDR2-mFc reduces polyclonal murine T cell proliferation. Naive $CD4^+$ T cells were isolated from two mouse strains, SJL or BALB/c, and activated in the presence of beads coated with anti-CD3 and anti-CD28, as described in Materials and Methods. The beads were also coated with the indicated concentrations of ILDR2-mFc or isotype control (mIgG2a). Cells were activated with the coated beads at a 1:1 ratio, and cell proliferation was evaluated by [^{3}H]thymidine incorporation after 72 h. (**E**) Soluble ILDR2-mFc reduces Ag-specific murine T cell activation. Naive $CD4^+$ T cells from DO11.1 mice were activated by 20 μg/ml $OVA_{323–339}$ peptide and coincubated with irradiated APCs at a 1:1 ratio in the presence of different concentrations of ILDR2-mFc or isotype control (mIgG2a). Proliferation was evaluated by [^{3}H] thymidine incorporation after 72 h. $^{**}p < 0.01$, $^{***}p < 0.001$, $^{\#}p < 0.0001$ versus empty vector.

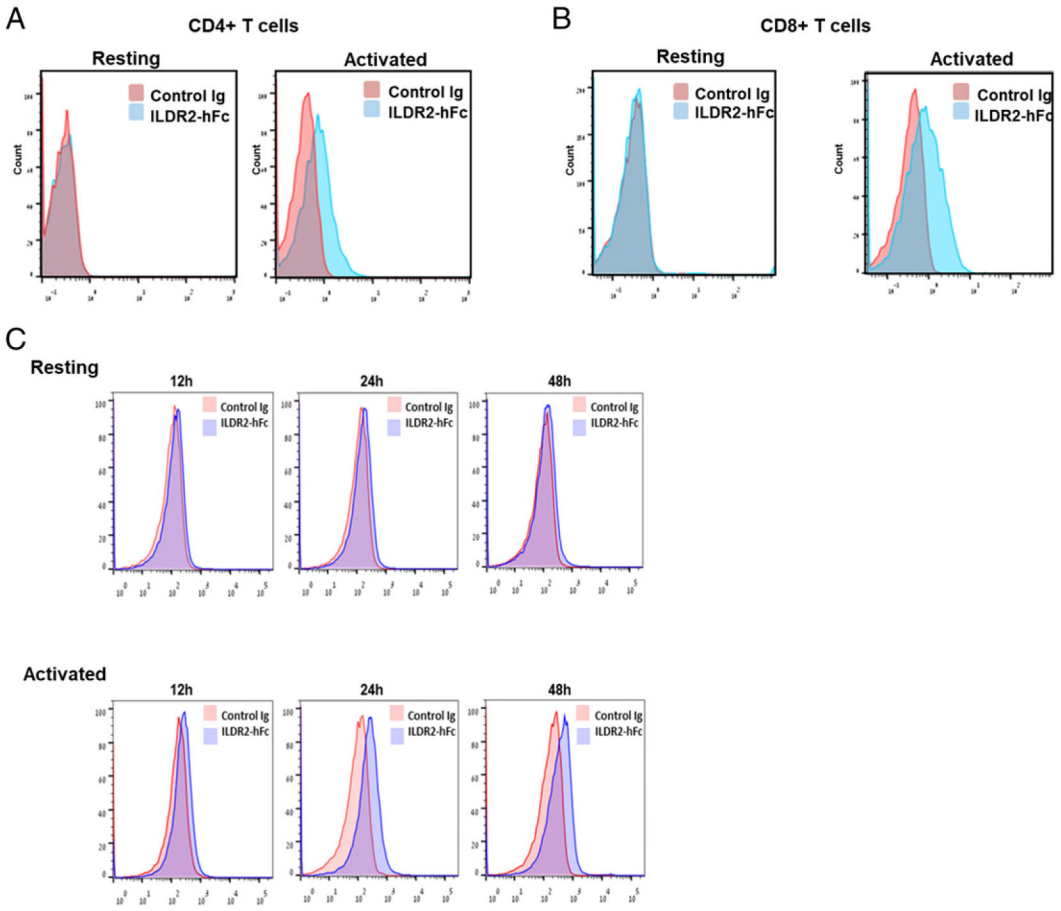

FIGURE 6.

ILDR2-Fc binds to activated T cells. Binding of ILDR2-hFc was analyzed on resting and activated human $CD4^+$ (**A**) and $CD8^+$ (**B**) T cells. Isolated human $CD4^+$ or $CD8^+$ T cells were left untreated or were stimulated with plate-bound anti-CD3 for 72 h, as described in Materials and Methods. Cells were incubated with ILDR2-hFc or isotype control (human IgG1; Synagis) at 100 μg/ml, followed by staining with PE-conjugated anti–human IgG Fc, and evaluated by flow cytometry. The results, shown as line graphs of ILDR2-hFc and isotype control (human IgG1) binding, are representative of two independent experiments. (**C**) Binding kinetics of ILDR2-mFc to resting and activated mouse $CD4^+$ T cells. $CD4^+$ $CD25^-$ T cells were isolated from BALB/C splenocytes and activated using plate-bound anti-CD3 and soluble anti-CD28, as described in Materials and Methods. Binding of biotinylated ILDR2-mFc and isotype control (mIgG2a) was tested at different time points of T cell activation and evaluated by flow cytometry. Results are shown as line graphs of ILDR2-mFc and isotype control (mIgG2a) binding.

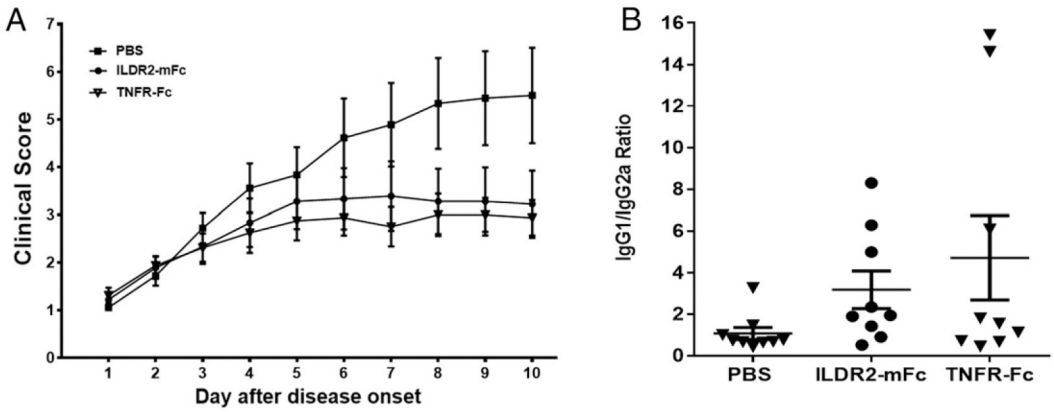

FIGURE 7.

Therapeutic effect of ILDR2-mFc in a CIA model of RA. (**A**) DBA/1 mice were immunized with bovine type II collagen in CFA and treated from the day of disease onset (day 1) with ILDR2-mFc (100 μg per mouse), TNFR-Fc (100 μg per mouse), or PBS (vehicle control), three times a week for 10 d. Average clinical scores (± SEM) are shown for $n = 8$ or 9 mice per group. Shown is one representative study of two. Data were analyzed using ANOVA, followed by the Dunnett posttest. PBS versus ILDR2-mFc, $p = 0.079$. PBS versus TNFR-Fc, $p = 0.047$. (**B**) At day 10 postdisease onset, serum levels of IgG1 and IgG2a anti-type II collagen Abs were evaluated by ELISA. Data are shown as the IgG1/IgG2a ratio. PBS versus ILDR2-mFc, $p = 0.041$. PBS versus TNFR-Fc, $p = 0.095$.

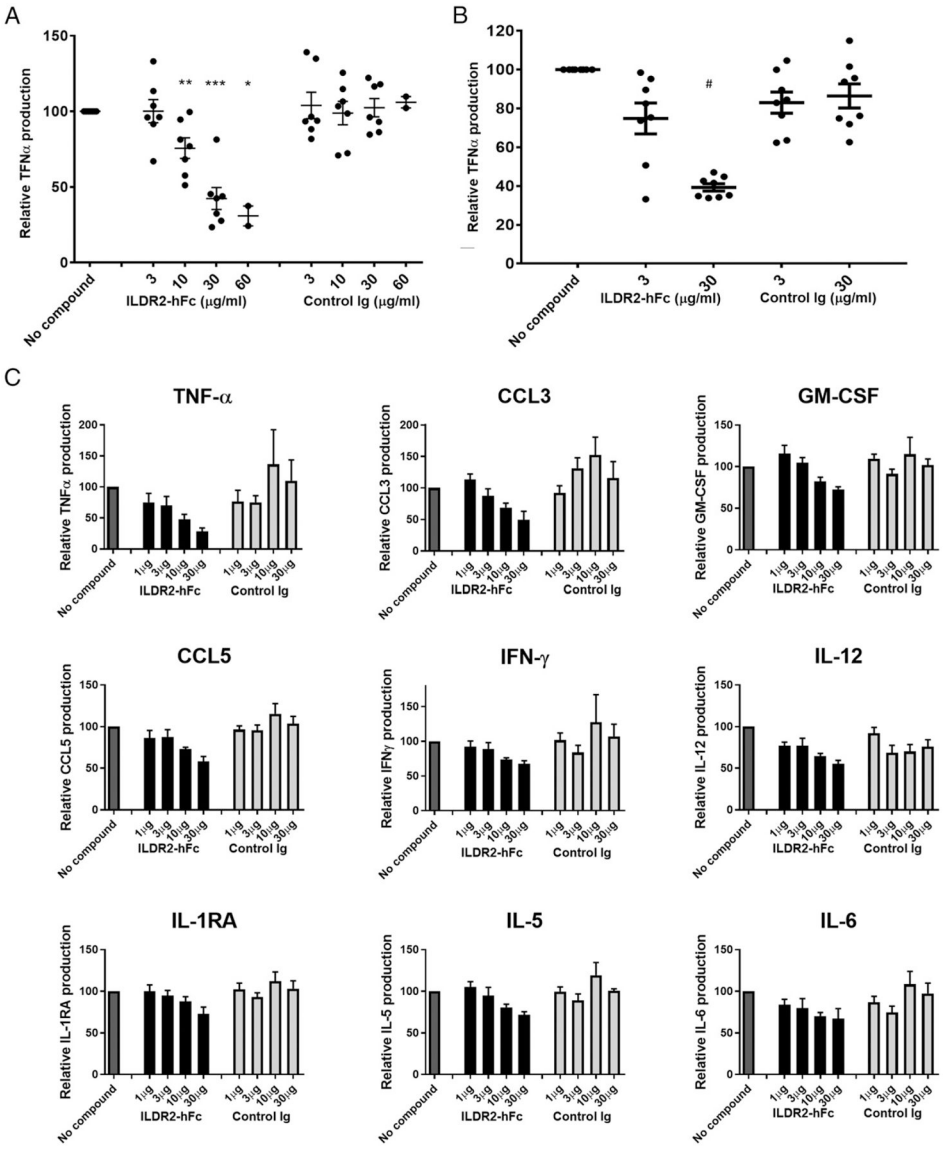

FIGURE 8.

ILDR2-hFc inhibits RA-related cytokines in translational autologous cocultures of "synovial-like" Tcks and monocyte-derived MΦs established from PBMCs of healthy controls or RA patients. ILDR2-hFc or isotype control (human IgG1) were added at the indicated concentrations to Tck and MΦ cocultures derived from healthy donors' PBMCs, as described in Materials and Methods. (**A**) After 24 h, supernatants were analyzed for TNF-α secretion by ELISA. (**B**) TNF-α secretion in MΦ and Tck cocultures derived from PBMCs of RA patients was evaluated by ELISA. (**C**) Supernatants from four of the donors in (A) were evaluated for secretion of additional RA-related cytokines and chemokines by Luminex. Cytokine values were normalized to those obtained in cultures without any added compound (No compound). Dots represent individual donors. Bars represent average ± SEM. $^{*}p < 0.05$, $^{**}p < 0.01$, $^{***}p < 0.001$, $^{\#}p < 0.0001$ versus the corresponding concentration of control Ig.

Table I.

Identity and similarity of ILDR2 IgV to other B7 family proteins

Protein IgV	Identity (%)	Similarity (%)
VISTA	19.5	34.0
PDL1	17.9	30.8
PDL2	17.5	24.4
B7H3	20.8	35.6
B7H4	16.9	27.1
ICOSL	17.2	35.2
CD80	16.4	31.5
CD86	15.3	27.0